VII International Conference on Computational Methods for Coupled Problems in Science and Engineering
COUPLED PROBLEMS 2017
M. Papadrakakis, E. Oñate and B. Schrefler (Eds)

ACCELERATION OF FLUID-STRUCTURE INTERACTION PROCEDURES BY ANTICIPATORY COUPLING

J.H. Seubers* **and A.E.P. Veldman†**

*†Computational Mechanics and Numerical Mathematics
University of Groningen
Nijenborgh 9, 9747 AG Groningen, The Netherlands
web page: http://www.rug.nl/fmns-research/cmnm
e-mail: *h.seubers@rug.nl, †a.e.p.veldman@rug.nl

Key words: Fluid-solid Interaction, Numerical Method, Strong Coupling, Added Mass

Abstract. Simulating the hydrodynamics of floating structures using a two-way partitioned coupling poses a major challenge when the coupling between the fluid and the structure is strong. The incompressibility of the fluid plays an important role, and leads to strong coupling when the ratio of so-called *added mass* to structural mass is considerate. Existing fluid-structure interaction procedures become less efficient in such cases, and can even become unstable. This paper proposes a coupling method that deals with the added-mass effect by anticipation, and remains stable and efficient at all times.

1 INTRODUCTION

Traditionally, multi-physics problems are classified as 'strongly' or 'weakly' interacting problems. From a physical perspective, the interaction is called *weak* if one subsystem dominates the behaviour of the coupled problem, and it is called *strong* if more than one of the subsystems 'equally contribute to the interaction' [1] or 'have an equal say' [2]. So the physical interaction strength is a scale running from a *one-way* hierarchy between systems to a *two-way* complementary interaction. An example of a hierarchy is the case of a very light particle (e.g. a ping-pong ball) in a large water wave: the motion of the ball follows completely from the motion of the wave. The wave is not affected by the presence of the ball. The exact opposite hierarchy occurs for heavy objects (e.g. a mammoth tanker) in quiet water: the flow of the water is completely determined by the motion of the ship. Of course, many real situations are somewhere in between these asymptotic cases, with *two-way* interaction between the subsystems: some feedback occurs from the water to the ship or from the particles to the water. The more feedback, the stronger the interaction.

In hydrodynamic applications with moving structures, a major factor affecting the interaction strength is the ratio of the *added mass* of fluid to the structural mass. In

the traditional formulation, where the fluid loads are imposed on the structure and the structural motions imposed on the fluid, higher added mass ratios increase the interaction strength. This effect makes simulation by traditional coupling methods of slender structures in large waves computationally expensive. The objective of the proposed method is to reduce the computation time for such applications.

Section 2 provides the motivation and physical background of fluid-structure coupling problems in marine hydrodynamics. The mathematical model of this problem is explained in section 3, which provides the necessary ingredients to analyze the coupling method. The new coupling method is introduced in section 4, where it is compared to existing methods. The properties of the new method are analyzed in section 5, and the results of some numerical experiments are discussed in section 6, leading to the conclusions in section 7.

2 PHYSICAL MODEL

Interactive simulations are important for predicting the behaviour of moored or free-floating ships or platforms in different operating conditions. On deck various operations may be performed that affect the load or inertia distribution of the vessel. The vessel responds not only to incoming waves but to the flow caused by its own motions as well: wave slamming, launching, green water events. The inertia of the water mass involved in these interacting flows is important for predicting the forces on the vessel. In other words, the inertia is an important feedback mechanism that leads to a strong coupling between the flow and the vessel motion.

The ship or platform, which will be referred to as the structure, is modelled as a rigid body with elastic mooring lines. The structure can have an arbitrary shape and can perform large but finite translations and rotations in three dimensions. It cannot deform or change in volume.

The water is modelled as an incompressible, viscous fluid with a free surface. Although the inviscid flow behaviour dominates the coupling, the vorticity and viscosity are included in order to show that the story remains essentially the same. The air flow is not modelled, a vacuum takes its place instead.

The interaction is modelled by conservation of momentum and geometric compatibility between the structure and fluid surface. Note that the topology and position of the fluid-structure interface can change in time.

3 MATHEMATICAL MODEL

Because of its flexibility, the partitioned approach will be adopted in this work. The partitioning cuts the system into two parts, a fluid subsystem (subscript $_f$) and a structure subsystem (subscript $_s$). The two subsystems with appropriate boundary conditions are represented as dynamical systems in a state-space representation, governed by the mass-

spring and Navier-Stokes equations respectively.

$$\mathrm{M}\ddot{\mathbf{x}} + \mathrm{K}\mathbf{x} = \mathrm{B}_s^T \mathbf{f}_s \qquad \rho\Omega\dot{\mathbf{u}} + \mathrm{G}\mathbf{p} + \rho\mathrm{C}(\mathbf{u})\mathbf{u} - \mu\mathrm{L}\mathbf{u} = \mathrm{B}_f^T \mathbf{f}_f \tag{1a}$$

$$\mathbf{y}_s = \mathrm{B}_s \ddot{\mathbf{x}} \qquad \mathbf{y}_f = \mathrm{B}_f \dot{\mathbf{u}} \tag{1b}$$

where $[\mathbf{x}, \mathbf{u}, \mathbf{p}]^T$ are the internal states of the fluid-structure system, $[\mathbf{y}_f, \mathbf{y}_s]^T$ are the motions at the component boundaries, and $[\mathbf{f}_f, \mathbf{f}_s]^T$ are the distributed loads at these boundaries. The domain where these variables live may deform over the time interval $[\mathrm{t}, \mathrm{t} + \Delta\mathrm{t}]$, see fig. 1.

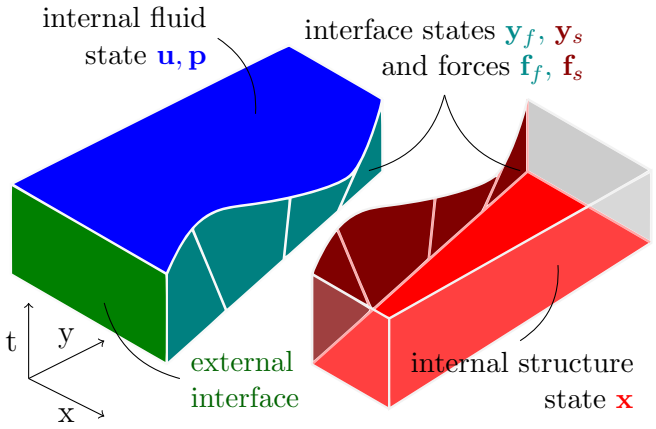

Figure 1: Model interface in space-time.

This mathematical model is not yet complete since the forces are not given. These are determined implicitly by two coupling criteria. The *kinematic* criterion requires that the motions on both sides of the fluid-structure interface are the same,

$$\delta\mathbf{y} := \mathbf{y}_f(t) - \mathbf{y}_s(t) = \mathbf{0}. \tag{2a}$$

The *dynamic* criterion expresses the balance of forces over the fluid-structure interface,

$$\sum \mathbf{f} := \mathbf{f}_f(t) + \mathbf{f}_s(t) = \mathbf{0}. \tag{2b}$$

Since the interaction is concerned with the variables that live on the interface, the internal states $[\mathbf{x}, \mathbf{u}, \mathbf{p}]^T$ are eliminated from the system by linearizing and substituting (1a) into (1b). This will lead to two operators that give the motions $\mathbf{y}$ in terms of the loads $\mathbf{f}$, the so-called Dirichlet-to-Neumann (DtN) operators A_f and A_s.

$$\mathbf{y}_f(t) = \mathbf{y}_f^0(t) + \mathrm{A}_f(t) * \mathbf{f}_f(t), \tag{3a}$$

$$\mathbf{y}_s(t) = \mathbf{y}_s^0(t) + \mathrm{A}_s(t) * \mathbf{f}_s(t). \tag{3b}$$

Together with the unloaded motions $\mathbf{y}^0_{f,s}$, these DtN operators completely describe the response of both subsystems to any load. Therefore, the difficulties of the interaction can be found by studying the properties of the DtN. It is easier to derive the DtN in the Laplace domain, where the time derivatives can be manipulated algebraically. To show how this is done, some simplified models are considered first.

3.1 Response of simplified models

Consider a cylinder on a spring, moving horizontally in a quiescent potential flow (fig. 2). The cylinders response is found by considering the equations of motion in the Laplace domain:

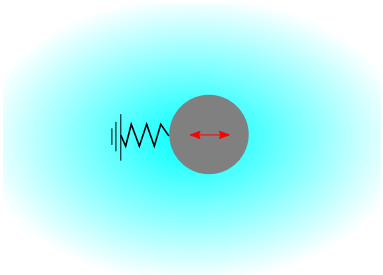

Figure 2: Spring-fixed cylinder moving in infinite potential flow

$$\begin{aligned} s^2\mathrm{m}\hat{x} + \mathrm{k}\hat{x} &= \hat{f}_s + \mathrm{m}(sx_0 + \dot{x}_0), \\ \hat{y}_s &= s^2\hat{x} - (sx_0 + \dot{x}_0). \end{aligned}$$

where m is the cylinder mass and k is the spring stiffness. This yields the response

$$\hat{y}_s = \left(\frac{s^2\mathrm{m}}{s^2\mathrm{m} + \mathrm{k}} - 1\right)(sx_0 + \dot{x}_0) + \left(\frac{s^2}{s^2\mathrm{m} + \mathrm{k}}\right)\hat{f}_s. \tag{4}$$

The DtN operator is recognized as $\hat{A}_s = \frac{s^2}{s^2m+k}$, which represents the acceleration of the cylinder due to an impulsive force at $t = 0$. The acceleration due to any other force can be found by convolution. In particular, the instantaneous acceleration due to a step force f_0 can be found from the initial value theorem,

$$y_s(t{=}0) = f_0 \lim_{s\to\infty} \hat{A}_s(s) = \frac{f_0}{\mathrm{m}}. \tag{5}$$

The fluid response is simply given by the added mass force. In summary, this simple interaction problem is governed by the two DtN operators

$$\hat{A}_s = \frac{s^2}{s^2\mathrm{m} + \mathrm{k}}, \qquad \hat{A}_f = \frac{1}{\mathrm{m}_a}. \tag{6}$$

3.2 Interactive response

Now recall the physical description of the ping-pong ball and the mammoth tanker. Since the feedback from the ping-pong ball on the water is small, we create an asymptotic expansion for the fluid motion $\hat{\mathbf{y}}_f(s)$ starting from the unforced fluid motion $\hat{\mathbf{y}}_f^0(s)$,

$$\hat{\mathbf{y}}_f = \hat{\mathbf{y}}_f^0 + \hat{\mathrm{A}}_f\hat{\mathrm{A}}_s^{-1}\big(\hat{\mathbf{y}}_s^0 - \hat{\mathbf{y}}_f^0\big) + \mathbf{O}(\hat{\epsilon}_f^2). \tag{7}$$

On the other hand, the asymptotic expansion for the mammoth tanker will start with the unforced vessel motion $\hat{\mathbf{y}}_{0s}(s)$, since the feedback from the water is small.

$$\hat{\mathbf{y}}_s = \hat{\mathbf{y}}_s^0 + \hat{\mathrm{A}}_s\hat{\mathrm{A}}_f^{-1}\big(\hat{\mathbf{y}}_f^0 - \hat{\mathbf{y}}_s^0\big) + \mathbf{O}(\hat{\epsilon}_s^2), \tag{8}$$

where the feedback strengths $\hat{\epsilon}_f$, $\hat{\epsilon}_s$ are measured by the disturbance of the motion

$$\hat{\epsilon}_f(s) = \left\|\hat{\mathrm{A}}_f(s)\hat{\mathrm{A}}_s^{-1}(s)\right\|, \qquad \hat{\epsilon}_s(s) = \left\|\hat{\mathrm{A}}_s(s)\hat{\mathrm{A}}_f^{-1}(s)\right\|. \tag{9}$$

At most one of these asymptotic expansions (7) or (8) will converge for a given problem, since $\hat{\epsilon}_f < 1$ implies $\hat{\epsilon}_s > 1$. Supposing that (8) converges, the motion will be given by

$$\hat{\mathbf{y}}_s = \hat{\mathbf{y}}_s^0 + \sum_{i=1}^{\infty}\big(\hat{\mathrm{A}}_s\hat{\mathrm{A}}_f^{-1}\big)^i\delta\hat{\mathbf{y}}^0 = \hat{\mathbf{y}}_s^0 + \big(\mathrm{I} - \hat{\mathrm{A}}_s\hat{\mathrm{A}}_f^{-1}\big)^{-1}\delta\hat{\mathbf{y}}^0 \tag{10}$$

In particular, this provides the interactive motion of the simplified models

$$\hat{y}_s = \hat{y}_s^0 + \sum_{i=1}^{\infty}\left(\frac{s^2\mathrm{m}_a}{s^2\mathrm{m}+\mathrm{k}}\right)^i\delta\hat{y}^0 = \hat{y}_s^0 + \left(\frac{s^2\mathrm{m}+\mathrm{k}}{s^2(\mathrm{m}-\mathrm{m}_a)+\mathrm{k}}\right)\delta\hat{y}^0. \tag{11}$$

Only for $\mathrm{m} > \mathrm{m}_a$, the roots of the denominator are in the left half plane, hence an oscillatory solution bounded by the initial disturbance δy^0 exists. In more complex cases, it could happen that neither expansion converges. In that case, both subsystems contribute equally: the physical interaction is strong. Therefore it makes sense to define the physical interaction strength as a product of the feedback strengths:

Definition 1. The physical *interaction strength* κ of the closed system (eqs. (1a), (1b), (2a) and (2b)) is a number between one and infinity, given by the initial value of the product of the feedback strengths,

$$\kappa = \lim_{s\to\infty}\hat{\epsilon}_f(s)\hat{\epsilon}_s(s)$$

This definition can be seen as the sensitivity of the responses for $t \to 0$. In the simplified scalar model (section 3.1) these sensitivities are the added mass ratio and its reciprocal,

$$\lim_{s\to\infty}\hat{\epsilon}_s = \left(\frac{m_a}{m}\right), \lim_{s\to\infty}\hat{\epsilon}_f = \left(\frac{m}{m_a}\right) \tag{12}$$

Generalizing this to systems, the sensitivities are the maximal and minimal eigenvalues of the matrix $\mathrm{A}_s\mathrm{A}_f^{-1}$. Note that κ is also the condition number of this matrix. Its eigenvalues can be interpreted physically as 'directional' added mass ratios, i.e. depending on the direction of the motion vector. When the interaction strength equals one, the coupled motion is simply a linear combination of the unforced motions $\mathbf{y}_f = (1-\alpha)\mathbf{y}_f^0 + \alpha\mathbf{y}_s^0$. In general however, this rarely occurs and interaction strengths may be higher. For rigid bodies floating in incompressible flow, it will be shown in section 5 that the interaction strength is still a function of mass ratios. But first, the performance of coupling algorithms will be directly related to the interaction strength in section 4.

4 NUMERICAL COUPLING METHODS

The basic coupling methods are related to the asymptotic expansions in eqs. (7) and (8). In marine hydrodynamics, the expansion (8) dominated by the ship motion is most natural, and it converges provided that the added mass is smaller than the ship mass,

$$\left\|\hat{\mathrm{A}}_s(s)\hat{\mathrm{A}}_f^{-1}(s)\right\| < 1 \qquad \text{i.e.} \quad \left|\frac{\mathrm{m}_a s^2}{\mathrm{m}s^2+\mathrm{k}}\right| < 1. \tag{13}$$

This coupling approach works well for weakly coupled problems, provided that the ship is indeed the dominant subsystem. If the ship is less dominant, it may be required to mix the approaches of the mammoth tanker and the ping-pong ball, using combinations of eqs. (7) and (8). Indeed modern domain decomposition approaches like FETI [3] are based on the difference between eqs. (7) and (8), $\delta\mathbf{y} = \mathbf{y}_f - \mathbf{y}_s$. This difference is iteratively reduced by splitting it over the two domains and then enforcing the dynamic criterion eq. (2b),

$$\delta\mathbf{y}_{i+1} = \delta\mathbf{y}_i + \big(\mathrm{A}_f + \mathrm{A}_s\big)\big(\alpha\mathrm{A}_f^{-1} + (1-\alpha)\mathrm{A}_s^{-1}\big)\delta\mathbf{y}_i, \tag{14}$$

where i is the iteration index. An early precursor to this approach is the semi-inverse method by Le Balleur (1978),

$$\delta\mathbf{y}_{i+1} = \delta\mathbf{y}_i - \alpha\big(\mathrm{A}_f + \mathrm{A}_s\big)\delta\mathbf{y}_i. \tag{15}$$

In both methods, a new force is estimated from $\delta\mathbf{y}$ and fed identically (but with opposite sign) to both subsystems to produce the new motions. These forces and motions are notated here as simple vectors, not as functions of time since eqs. (14) and (15) are steady state methods. An extension of the semi-inverse method that operates on time series of forces and motions is known as waveform relaxation [4]. In each iteration, both subsystems are integrated in time based on an estimated force series. The difference in the resulting motion series are multiplied by the relaxation parameter α to produce a new force estimate, exactly as in (15).

FETI, semi-inverse and waveform relaxation methods can all be seen as local preconditioners for the kinematic criterion eq. (2a), see fig. 3. For a suitable range of α, such methods can deal with strongly coupled problems. However, their convergence ($\delta\mathbf{y} \to 0$) slows down as the coupling strength increases.

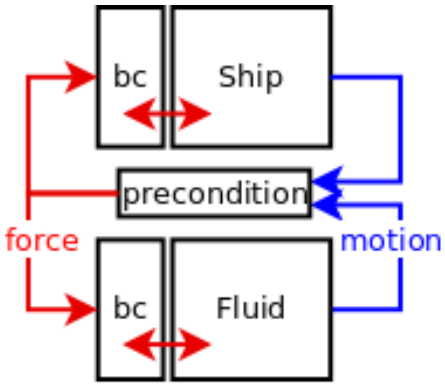

Figure 3: Preconditioning schemes: semi-inverse, FETI, waveform relaxation

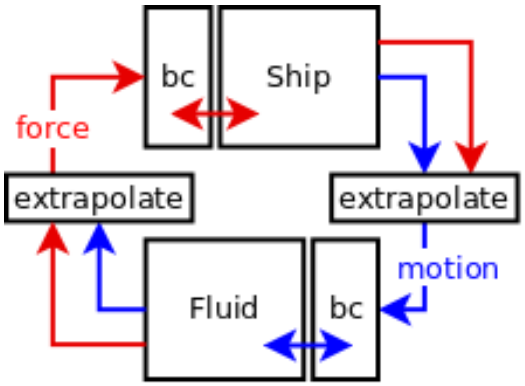

Figure 4: Extrapolation schemes: Gauss-Seidel, IQN, IBQN, manifold mapping

Another family of methods for strongly coupled problems is based on the Gauss-Seidel approach (fig. 4). Instead of applying the coupling criteria (2) directly, the expansion (8) is modified by introducing extrapolation steps. The simplest type of extrapolation is under-relaxation,

$$\mathbf{y}_{i+1} = \mathbf{y}_i + \alpha \mathrm{A}_s \mathrm{A}_f^{-1} \delta \mathbf{y}_i. \tag{16}$$

This method will again converge for suitable α, albeit slower when the interaction becomes stronger. In fact, even for the optimal choice in α, the performance of this method deteriorates linearly with the coupling strength.

4.1 Anticipatory coupling

The quasi-simultaneous method [5] however, avoids the need for extrapolation or relaxation by reformulating the original problem to an equivalent one with reduced coupling strength. This is achieved by replacing the system of coupling conditions (2) by an equivalent system,

$$\mathbf{y}_f + \mathrm{D}_i \mathbf{f}_f = \mathbf{y}_s - \mathrm{D}_i \mathbf{f}_s, \tag{17a}$$

$$\mathbf{f}_f + \mathbf{f}_s = \mathbf{0}. \tag{17b}$$

Note that eq. (17a) is formed by eq. (2a) plus an arbitrary operator D_i times eq. (2b).

Since eq. (2a) was previously used as a boundary condition for the fluid, this simply amounts to a more general boundary condition. A suitable choice of the operator D_i would contain some approximate physics of the structure. In the anticipatory coupling method, we choose D_i as the instantaneous approximation of the structure:

$$D_i = \lim_{s \to \infty} \hat{A}_s. \tag{18}$$

This choice is motivated as follows. The approximation (18) is

- easy to obtain, only the inertia properties such as the mass of the structure are needed.
- exact at $t = 0$, so zero-stability of the subsystems implies zero-stability of the coupling.
- physically consistent, no artificial physics are introduced into the problem.

The difference between D_i and A_s will produce a finite error in the solution at finite timesteps, but this error can be controlled by varying the timestep size, or resorting to any of the above families of coupling methods. The anticipatory algorithm thus takes the following steps:

1. Initialize structural motion $\mathbf{y}_s^{old}$ and loads $\mathbf{f}_s^{old}$ from previous timestep
2. Predict fluid velocities $\tilde{\mathbf{u}}$ due to convection and diffusion
3. Move the geometry based on the structural motion $\mathbf{y}_s^{old}$
4. Compute new fluid force $\mathbf{f}_f^{new}$ in Poisson equation with anticipative condition (17a)
$$\tilde{\mathbf{y}}_f + \mathrm{D}_i \mathbf{f}_f^{new} = \mathbf{y}_s^{old} - \mathrm{D}_i \mathbf{f}_s^{old}$$
5. Compute new structural response $\mathbf{y}_s^{new}$ with dynamic condition (2b)
$$\mathbf{f}_s^{new} = \mathbf{f}_f^{new}$$
6. Enforce the kinematic condition (2a) $\mathbf{y}_f^{new} = \mathbf{y}_s^{new}$ (discarding $\tilde{\mathbf{y}}_f$)
7. Correct fluid velocities $\mathbf{u}$ and update the free-surface position
8. Go to the next timestep

To see the effect of the anticipative condition, it is illustrative to look at the simplified model from section 3.1 again. In this example, the modified Dirichlet-to-Neumann maps become

$$\hat{\mathrm{A}}_f(s) + \mathrm{D}_i = \frac{1}{\mathrm{m}_a} + \mathrm{d}_i, \tag{19a}$$

$$\hat{\mathrm{A}}_s(s) - \mathrm{D}_i = \frac{s^2}{s^2\mathrm{m} + \mathrm{k}} - \mathrm{d}_i. \tag{19b}$$

Although these are only a scalar equation, it is clear that this affects the asymptotic expansion in general as

$$\hat{\mathbf{y}}_s = \hat{\mathbf{y}}_s^0 + (\hat{\mathrm{A}}_s - \mathrm{D}_i)(\hat{\mathrm{A}}_f + \mathrm{D}_i)^{-1}\delta\hat{\mathbf{y}}^0 + \mathbf{O}(\hat{\epsilon}_s^2), \tag{20}$$

hence the feedback strength becomes

$$\hat{\epsilon}_s(s) = \left| \frac{s^2\mathrm{m}_a}{s^2\mathrm{m} + \mathrm{k}} \, \frac{1 - \mathrm{d}_i\mathrm{m}}{1 + \mathrm{d}_i\mathrm{m}_a} + O(s^{-2}) \right|. \tag{21}$$

Therefore any choice $0 < \mathrm{d}_i^{-1} < 2m$ makes $\hat{\epsilon}_s(\infty) < 1$, and then the expansion (8) converges, at least for small enough time intervals.

5 ANALYSIS OF THE METHOD

To extend the convergence result for the simple models to the Navier-Stokes and mass-spring model, we will take the following steps.

- Obtain the DtN operators for the Navier-Stokes and mass-spring models
- Choose D_i based on the instantaneous response from the DtN operators
- Show that the anticipative scheme has a feedback of order $s^{-1} \sim \Delta t$

5.1 Linearized DtN operators

The discrete mass-spring model in (1a) for the structure is transformed into the Laplace domain,

$$(s^2\mathrm{M} + \mathrm{K})\hat{\mathbf{x}} = \mathrm{B}_s^T\hat{\mathbf{f}}_s + \mathrm{M}(s\mathbf{x}_0 + \dot{\mathbf{x}}_0) \tag{22a}$$

$$\hat{\mathbf{y}}_s = s^2\mathrm{B}_s\hat{\mathbf{x}} - \mathrm{B}_s(s\mathbf{x}_0 + \dot{\mathbf{x}}_0). \tag{22b}$$

By eliminating the internal unknown $\hat{\mathbf{x}}$ by the same procedure used in eq. (4) the response of the structure is found

$$\hat{\mathbf{y}}_s = \hat{\mathbf{y}}_s^0 + \mathrm{B}_s\big(\mathrm{M} + s^{-2}\mathrm{K}\big)^{-1}\mathrm{B}_s^T\hat{\mathbf{f}}_s. \tag{23}$$

The treatment of the Navier-Stokes model in (1a) contains an additional step, since both $\hat{\mathbf{p}}$ and $\hat{\mathbf{u}}$ must be eliminated. Starting from the basic equations linearized around $\mathbf{u}_0$ in the Laplace domain

$$-\mathrm{G}^T\hat{\mathbf{u}} = \mathbf{0} \tag{24a}$$

$$(s\rho\Omega + \rho\mathrm{C}(\mathbf{u}_0) - \mu\mathrm{L})\hat{\mathbf{u}} = \mathrm{B}_f^T\hat{\mathbf{f}}_f - \mathrm{G}\hat{\mathbf{p}} + \rho\Omega\mathbf{u}_0 \tag{24b}$$

$$\hat{\mathbf{y}}_f = s\mathrm{B}_f\hat{\mathbf{u}} - \mathrm{B}_f\mathbf{u}_0, \tag{24c}$$

the pressure is eliminated first by using the continuity equation (24a). Denoting the action of convection and diffusion by $\hat{\mathrm{T}}^{-1} = \mathrm{I} + (s\Omega)^{-1}(\mathrm{C}(\mathbf{u}_0) - \nu\mathrm{L})$, an analog for the pressure Poisson equation is found

$$\left(\mathrm{G}^T\hat{\mathrm{T}}\Omega^{-1}\mathrm{G}\right)\hat{\mathbf{p}} = \mathrm{G}^T\hat{\mathrm{T}}\Omega^{-1}\mathrm{B}_f^T\hat{\mathbf{f}}_f + \mathrm{G}^T\hat{\mathrm{T}}\rho\mathbf{u}_0. \tag{25}$$

The momentum (24b) and pressure (25) equations are then used to eliminate $\hat{\mathbf{u}}$ and $\hat{\mathbf{p}}$ from (24c). What remains is the response of the fluid to the imposed loads,

$$\begin{aligned}\hat{\mathbf{y}}_f &= \frac{1}{\rho}\mathrm{B}_f\hat{\mathrm{T}}\Omega^{-1}\left(\mathrm{B}_f^T\hat{\mathbf{f}}_f - \mathrm{G}\hat{\mathbf{p}}\right) + \mathrm{B}_f(\hat{\mathrm{T}}\mathbf{u}_0 - \mathbf{u}_0)\\ &= \frac{1}{\rho}\mathrm{B}_f\left(\mathrm{I} + \hat{\mathrm{T}}\Omega^{-1}\Delta\right)\hat{\mathrm{T}}\Omega^{-1}\mathrm{B}_f^T\hat{\mathbf{f}}_f + \hat{\mathbf{y}}_f^0\end{aligned} \tag{26}$$

where $\Delta = -\mathrm{G}\left(\mathrm{G}^T\mathrm{T}\Omega^{-1}\mathrm{G}\right)^{-1}\mathrm{G}^T$ is the global transport of fluid volume required to satisfy the incompressibility constraint. In summary, the interaction problem eqs. (1a), (1b), (2a) and (2b) is governed by the two DtN operators

$$\hat{\mathrm{A}}_s = \mathrm{B}_s\big(\mathrm{M} + s^{-2}\mathrm{K}\big)^{-1}\mathrm{B}_s^T, \qquad \hat{\mathrm{A}}_f = \frac{1}{\rho}\mathrm{B}_f\left(\mathrm{I} + \hat{\mathrm{T}}\Omega^{-1}\Delta\right)\hat{\mathrm{T}}\Omega^{-1}\mathrm{B}_f^T. \tag{27}$$

5.2 Instantaneous response

The fluid and structure should be aware of each others most immediate response, so they can anticipate what will happen. This is achieved by choosing boundary conditions that approximate the actual response, i.e. that approximate the DtN operators. The approximation here is crucial, since the full nonlinear dynamical DtNs are practically too expensive to use. For coupled simulations with finite time-steps, the instantaneous response would be a good choice of boundary condition. Hereto, we define a splitting of eq. (27) into an instantaneous part $\mathrm{A}_\cdot^0$ and a time dependent part $\hat{\mathrm{A}}_\cdot^+(s)$, such that $\hat{\mathrm{A}}_\cdot(s) = \mathrm{A}_\cdot^0 + \hat{\mathrm{A}}_\cdot^+(s)$.

$$\mathrm{A}_s^0 = \lim_{s\to\infty}\hat{\mathrm{A}}_s = \mathrm{B}_s\mathrm{M}^{-1}\mathrm{B}_s^T, \qquad \mathrm{A}_f^0 = \lim_{s\to\infty}\hat{\mathrm{A}}_f = \frac{1}{\rho}\mathrm{B}_f\left(\mathrm{I} + \Omega^{-1}\Delta\right)\Omega^{-1}\mathrm{B}_f^T. \tag{28}$$

These are the equivalents of the structural mass and added mass from eq. (6). In step 4 of the algorithm, the strong coupling between these masses is ensured by choosing $D_i = \mathrm{A}_s^0 - \hat{\mathrm{A}}_f^+$ in the fluid boundary condition. The fluid system therefore becomes

$$\begin{cases} \hat{\mathbf{y}}_f &= \hat{\mathbf{y}}_f^0 + \hat{\mathrm{A}}_f\hat{\mathbf{f}}_f \\ \hat{\mathbf{y}}_f + \left(\mathrm{A}_s^0 - \hat{\mathrm{A}}_f^+\right)\hat{\mathbf{f}}_f &= \hat{\mathbf{y}}_s - \left(\mathrm{A}_s^0 - \hat{\mathrm{A}}_f^+\right)\hat{\mathbf{f}}_s \end{cases} \tag{29}$$

Note that this is equivalent to

$$\left(\mathrm{A}_s^0 + \mathrm{A}_f^0\right)\hat{\mathbf{f}}_f = \hat{\mathbf{y}}_s^0 - \hat{\mathbf{y}}_f^0 + \left(\hat{\mathrm{A}}_s^+ + \hat{\mathrm{A}}_f^+\right)\hat{\mathbf{f}}_s \tag{30}$$

To solve this set of equations for the fluid force, the structural mass A_s^0 and the added mass A_f^0 must be solved implicitly, while the nonlinear convection-diffusion and spring terms in $\hat{\mathrm{A}}_s^+$ and $\hat{\mathrm{A}}_f^+$ are integrated explicitly. Since both A_f^0 and A_s^0 are symmetric positive (semi)definite, the existing pressure solver can be used to solve this system.

5.3 Consistency and stability

By design, the new fluid system (29) is consistent with the original one. Hence it remains to show that the fluid-structure iteration based on eqs. (17a) and (17b) with this choice of D_i is stable. The expansion obtained by substituting eq. (30) into eq. (3b) is

$$\hat{\mathbf{y}}_s = \hat{\mathbf{y}}_s^0 + (\hat{\mathrm{A}}_s^+ + \hat{\mathrm{A}}_f^+)(\mathrm{A}_f^0 + \mathrm{A}_s^0)^{-1}\delta\hat{\mathbf{y}}^0 + \mathbf{O}(\hat{\epsilon}^2). \tag{31}$$

This iteration is stable if $\left|(\hat{\mathrm{A}}_s^+ + \hat{\mathrm{A}}_f^+)(\mathrm{A}_f^0 + \mathrm{A}_s^0)^{-1}\right| < 1$.

Using a power series expansion of $\hat{\mathrm{A}}_f^+$ and $\hat{\mathrm{A}}_s^+$, it can be shown that these are of order s^{-1} and s^{-2} respectively. Hence any zero-stable time integration scheme can be used with the anticipatory method, resulting in a stable and convergent interaction scheme.

6 RESULTS AND DISCUSSION

Two test cases are presented here to show the performance of the method. The first is a simulation of a lifeboat dropped into a breaking wave. The lifeboat has an average density of $320kg/m^3$, the water a density of $1025kg/m^3$. It is dropped from $37m$ height and hits the water at $t = 2.5s$. The added mass varies greatly over time during the impact, as the boat enters the water and a larger part of the wave has to respond. It is clear that the relaxation-based method (16) is sensitive to this ratio, as the workload increases during the entry phase. The anticipative method (31) however remains efficient regardless of the added-mass ratio, as the boundary condition inside the wave predicts the boat motion. The workload is reduced by a factor around 10 for the complete simulation.

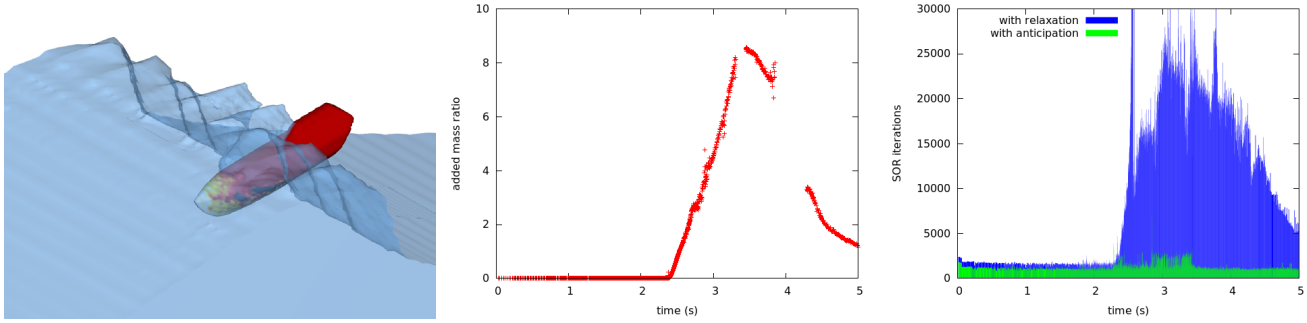

Figure 5: Simulation of a lifeboat dropped into a breaking wave. Left: the situation at $t = 3.0$. Middle: variation of effective added-mass ratio over time. Right: the workload for the simulation corresponds to the area under the curve.

The second test case is a tension-leg platform in a long-crested wave. The wave is a nonlinear 5th-order Stokes wave with a height of $23cm$. Since the variations around the waterline are small compared to the size of the platform, the added-mass ratio is relatively constant. Even for this moderate added-mass ratio however, the anticipative method outperforms the relaxation-based method by a factor 2.5 to 3.0.

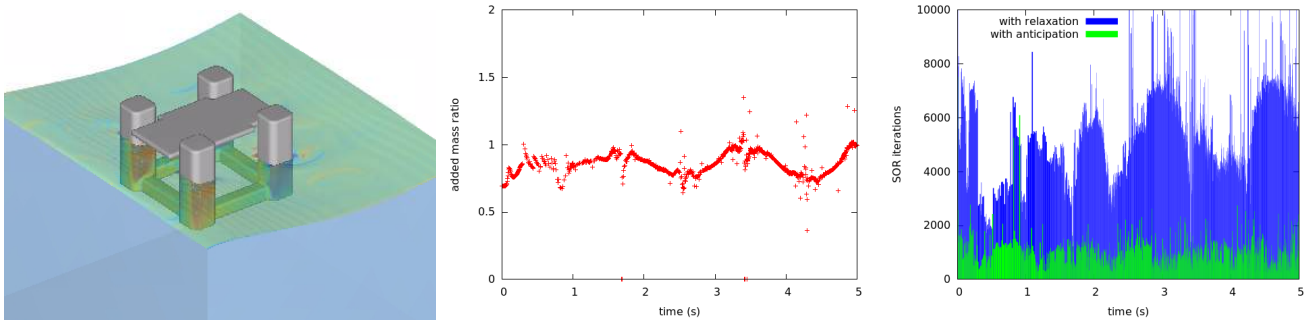

Figure 6: Simulation of tension-leg platform in Stokes-5 wave. Left: platform in wave (tendons not shown). Middle: variation of effective added-mass ratio over time. Right: the workload for the simulation corresponds to the area under the curve.

7 CONCLUSIONS

Analysis of fluid-structure interaction showed that the coupling strength is directly related to the added-mass ratio. This affected the existing partitioned coupling schemes based on the exchange of loads and motions: A stronger coupling with a higher range of added-mass ratios led to loss of performance in these traditional coupling schemes. The anticipatory coupling scheme was shown to be robust and insensitive to the added-mass ratio, using two test cases relevant to marine hydrodynamics. Additionally, theory on the stability and convergence of the method was derived for the general coupling of the Navier-Stokes equations with a mass-spring system.

This work is part of the research programme Maritime2013 with project number 13267, which is (partly) financed by the Netherlands Organisation for Scientific Research (NWO).

REFERENCES

[1] H. Bijl, A. H. van Zuijlen, and S. Bosscher. “Two level algorithms for partitioned fluid-structure interaction computations”. In: *ECCOMAS CFD* (2006).

[2] A. E. P. Veldman. “A simple interaction law for viscous-inviscid interaction”. In: *Journal of engineering mathematics* 65.4 (2009), pp. 367–383. ISSN: 0022-0833.

[3] C. Farhat and F.-X. Roux. “A method of finite element tearing and interconnecting and its parallel solution algorithm”. In: *International journal for numerical methods in engineering* 32.6 (1991), pp. 1205–1227.

[4] E. Lelarasmee, A. E. Ruehli, and A. L. Sangiovanni-Vincentelli. “Waveform relaxation method for time-domain analysis of large scale integrated circuits.” In: *IEEE transactions on computer-aided design of integrated circuits and systems* CAD-1.3 (1983), pp. 131–145.

[5] A. E. P. Veldman. “New, quasi-simultaneous method to calculate interacting boundary layers”. In: *AIAA journal* 19.1 (1981).